Report

Cell Reports

Thymidine Catabolism as a Metabolic Strategy for Cancer Survival

Graphical Abstract

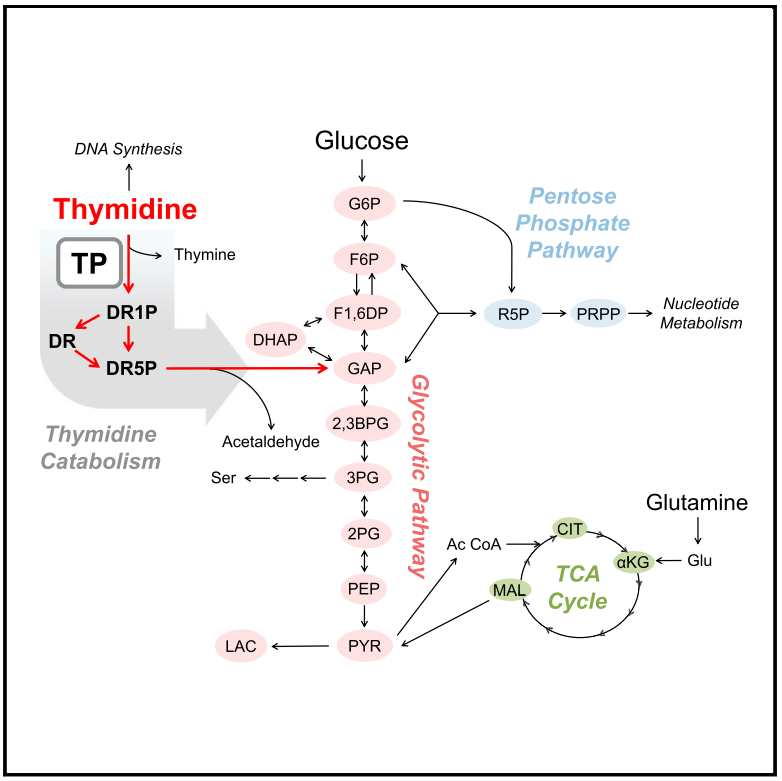

Authors

Sho Tabata, Masatatsu Yamamoto, Hisatsugu Goto, ..., Tomoyoshi Soga, Tatsuhiko Furukawa, Shin-ichi Akiyama

Correspondence

tabata@ttck.keio.ac.jp (S.T.), furukawa@m3.kufm.kagoshima-u.ac.jp (T.F.), akiyama19450331@gmail.com (S.-i.A.)

In Brief

Tabata et al. find that thymidine phosphorylase (TP)-mediated thymidine catabolism can supply carbon to the glycolytic pathway in mammalian cells. In TP-expressing cancer cells, thymidine contributes to cell survival under nutrient starvation.

Highlights

- Thymidine catabolism can supply carbon for glycolysis
- TP-expressing cancer cells are resistant to nutrient starvation
- Thymidine-derived metabolites enter glycolysis in a physiological context
- Thymidine is catabolized to lactate in TP-expressing tumor xenografts

Tabata et al., 2017, Cell Reports *19*, 1313–1321
May 16, 2017
http://dx.doi.org/10.1016/j.celrep.2017.04.061

Cell Reports
Report

Thymidine Catabolism as a Metabolic Strategy for Cancer Survival

Sho Tabata,[1,8,*] Masatatsu Yamamoto,[2] Hisatsugu Goto,[3] Akiyoshi Hirayama,[1] Maki Ohishi,[1] Takuya Kuramoto,[3] Atsushi Mitsuhashi,[3] Ryuji Ikeda,[4] Misako Haraguchi,[5] Kohichi Kawahara,[2] Yoshinari Shinsato,[2] Kentaro Minami,[2] Atsuro Saijo,[3] Masaki Hanibuchi,[3] Yasuhiko Nishioka,[3] Saburo Sone,[3] Hiroyasu Esumi,[6] Masaru Tomita,[1] Tomoyoshi Soga,[1] Tatsuhiko Furukawa,[2,*] and Shin-ichi Akiyama[7,*]

[1]Institute for Advanced Biosciences, Keio University, 246-2 Mizukami, Kakuganji, Tsuruoka, Yamagata 997-0052, Japan
[2]Department of Molecular Oncology, Graduate School of Medical and Dental Sciences, Kagoshima University, 8-35-1 Sakuragaoka, Kagoshima 890-8544, Japan
[3]Department of Respiratory Medicine and Rheumatology, Institute of Biomedical Sciences, Tokushima University Graduate School, 3-18-15 Kuramoto-cho, Tokushima 770-8503, Japan
[4]Department of Clinical Pharmacy and Pharmacology, Graduate School of Medical and Dental Sciences, Kagoshima University, 8-35-1 Sakuragaoka, Kagoshima 890-8544, Japan
[5]Department of Biochemistry and Molecular Biology, Graduate School of Medical and Dental Sciences, Kagoshima University, 8-35-1 Sakuragaoka, Kagoshima 890-8544, Japan
[6]Clinical Research, Research Institute for Biomedical Sciences, Tokyo University of Science, 2641 Yamazaki, Noda, Chiba 278-0022, Japan
[7]Clinical Research Center, National Kyushu Cancer Center, 3-1-1 Notame Minami-ku, Fukuoka 811-1395, Japan
[8]Lead Contact
*Correspondence: tabata@ttck.keio.ac.jp (S.T.), furukawa@m3.kufm.kagoshima-u.ac.jp (T.F.), akiyama19450331@gmail.com (S.-i.A.)
http://dx.doi.org/10.1016/j.celrep.2017.04.061

SUMMARY

Thymidine phosphorylase (TP), a rate-limiting enzyme in thymidine catabolism, plays a pivotal role in tumor progression; however, the mechanisms underlying this role are not fully understood. Here, we found that TP-mediated thymidine catabolism could supply the carbon source in the glycolytic pathway and thus contribute to cell survival under conditions of nutrient deprivation. In TP-expressing cells, thymidine was converted to metabolites, including glucose 6-phosphate, lactate, 5-phospho-α-D-ribose 1-diphosphate, and serine, via the glycolytic pathway both in vitro and in vivo. These thymidine-derived metabolites were required for the survival of cells under low-glucose conditions. Furthermore, activation of thymidine catabolism was observed in human gastric cancer. These findings demonstrate that thymidine can serve as a glycolytic pathway substrate in human cancer cells.

INTRODUCTION

Thymidine phosphorylase (TP) catalyzes the reversible phosphorolysis of thymidine to thymine and 2-deoxy-D-ribose 1-phosphate (DR1P). We have previously demonstrated that TP is identical to the angiogenic factor platelet-derived endothelial cell growth factor (PD-ECGF) (Furukawa et al., 1992). TP expression in various malignant tumors is higher than in adjacent non-neoplastic tissues (Takebayashi et al., 1996b), and a poor prognosis is associated with TP-positive versus TP-negative colon and differentiated gastric carcinomas (Shimaoka et al., 2000; Takebayashi et al., 1996a).

2-Deoxy-D-ribose (DR) is a downstream mediator of TP function; it also shows angiogenic activity and shares some functions with TP (Haraguchi et al., 1994). DR affects endothelial cell migration through activation of the integrin downstream signaling pathway (Hotchkiss et al., 2003). Conversely, rapamycin completely abrogates DR-induced cell migration and angiogenesis via inhibition of DR-induced p70/s6 kinase activation (Seeliger et al., 2004). DR and DR1P are enzymatically converted to 2-deoxy-D-ribose 5-phosphate (DR5P) (Hoffee, 1968); both DR1P and DR5P accumulate at high levels in TP-overexpressing cells, which extensively secrete DR (Bijnsdorp et al., 2010). However, the functional cascades induced by TP and DR remain largely unknown.

RESULTS

Growth Advantage Conferred by TP under Low-Nutrient Conditions

Animal models and clinical studies have shown that TP is involved in cancer cell growth, invasion, and metastasis (Akiyama et al., 2004). We found that, in a xenograft mouse model, TP-overexpressing human epidermoid carcinoma KB (KB/TP) cells demonstrated a growth advantage over TP-negative control vector-transfected (KB/CV) cells and that KB/TP cell growth was suppressed by TPI, a TP enzymatic inhibitor (Matsushita et al., 1999). Figure S1A and Figure 1A show the growth of KB cells in 10% fetal bovine serum (FBS) and serum-free medium, respectively. Under serum-free conditions, both cell types had a similar growth rate until 2 days, whereas the growth of KB/CV cells, but not KB/TP cells, was suppressed thereafter. TPI lowered the KB/TP growth rate comparable with

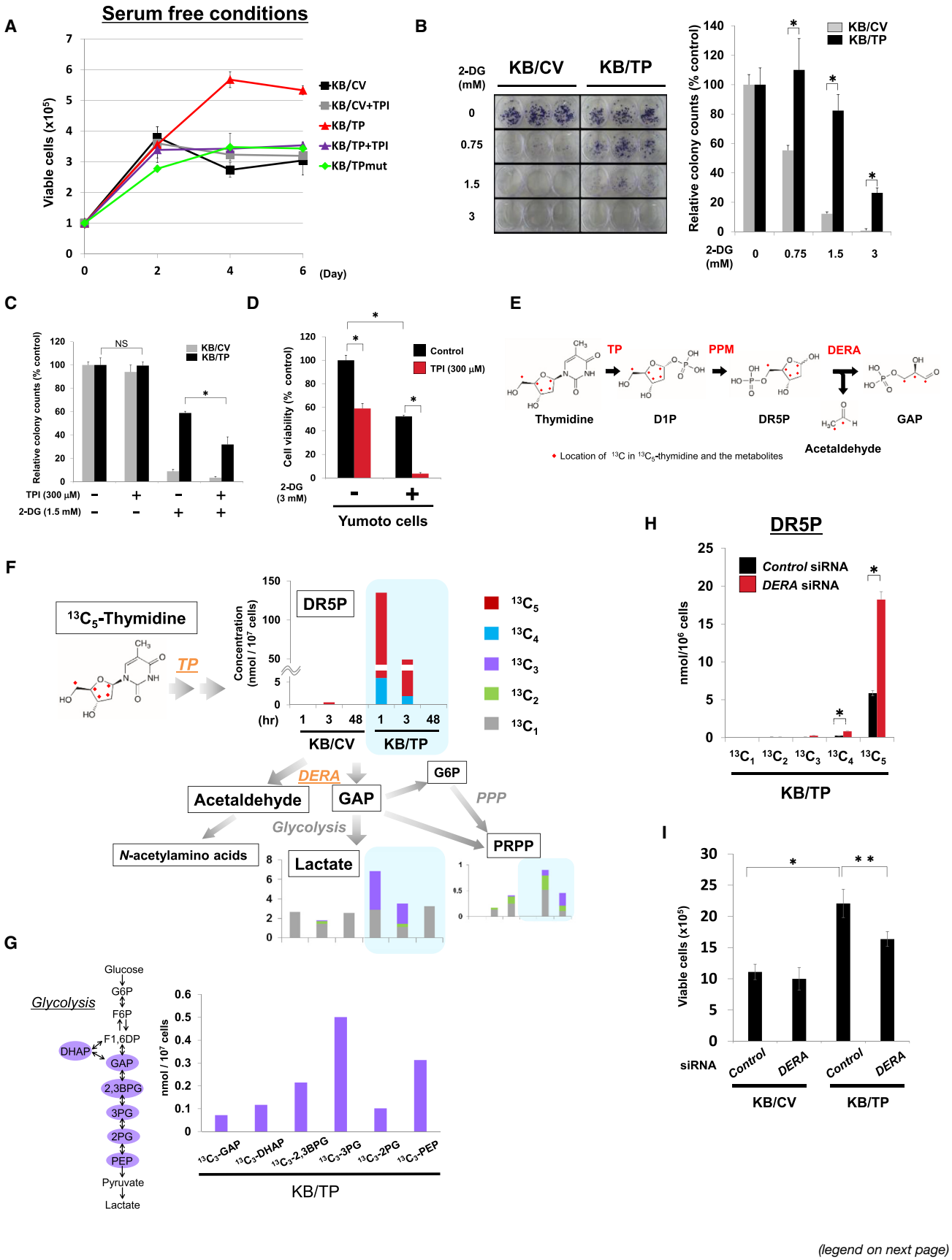

(legend on next page)

those of KB/CV and KB/TPmut cells, which express an enzymatic activity-deficient mutant TP (Figure 1A). The sub-G1 fraction, a measure of apoptosis, was considerably lower in KB/TP cells than in KB/CV cells under serum-free conditions (Figure S1B). These results suggested that TP enzymatic activity provides a growth advantage for KB/TP cells under low-nutrition conditions.

2-Deoxy-D-glucose (2-DG), a glucose analog, inhibits phosphohexose isomerase and restricts glucose availability. In a colony formation assay, KB/TP cells were more resistant to 2-DG than KB/CV cells (Figure 1B), as were TP-overexpressing (EJ/TP) versus control-transfected (EJ/CV) human bladder carcinoma EJ cells (Figure S1C). Although 300 μM TPI did not affect KB/CV and KB/TP colony formation, it significantly decreased KB/TP colony number in the presence of 1.5 mM 2-DG (Figure 1C). TPI also considerably enhanced the cytotoxic effect of 2-DG against intrinsically TP-expressing human cervical cancer Yumoto cells (Figure 1D). We also assessed the consumption levels of glucose and glutamine in KB cells under serum-free conditions (Figure S1D). Glucose and glutamine levels in KB/TP cell culture medium were similar to those in KB/CV cell culture medium. These results suggest that TP contributes to cell growth specifically under glucose deprivation conditions and that the growth advantage in KB/TP cells is not related to glucose and glutamine uptake.

Thymidine Catabolism as the Carbon Source for Glycolysis in TP-Expressing Cancer Cells

In certain prokaryotes, phosphopentose mutase (PPM) converts thymidine-derived DR1P to DR5P, which is then converted to glyceraldehyde 3-phosphate (GAP) and acetaldehyde by DR5P aldolase (DERA) (Hoffee, 1968). Given that GAP is an intermediate in the glycolytic pathway and pentose phosphate pathway (PPP), we hypothesized that the activation of thymidine catabolism by TP could supply the carbon source for those pathways. However, the thymidine catabolic pathway in mammalian cells remains unclarified. We examined whether 1′,2′,3′,4′,5′-$^{13}C_5$-thymidine ($^{13}C_5$-thymidine) metabolites (Figure S2A) enter the glycolytic pathway and PPP in KB/TP cells. An expected $^{13}C_5$-thymidine catabolic pathway is shown in Figure 1E. The time-dependent accumulation of ^{13}C-metabolites (DR5P, lactate, and 5-phospho-α-D-ribose 1-diphosphate [PRPP]) in KB/TP cells treated with $^{13}C_5$-thymidine were determined (Figure 1F). Figure S2B shows the enrichment of ^{13}C-metabolites in the same experiments. We also detected $^{13}C_1$- and $^{13}C_2$-labeled metabolites in the lactate and PRPP of KB/CV cells, which were expected to be natural. Because the limited ^{13}C-metabolites were recognized (Figure 1F), we further examined whether the other ^{13}C-labeled glycolytic intermediates could be detected in KB/TP cells when the experimental conditions were changed. $^{13}C_3$-G6P was detected as early as 10 min after $^{13}C_5$-thymidine addition (Figure S2C). In KB/TP cells treated with $^{13}C_5$-thymidine for 1 hr under 80%–90% confluent conditions after the cells had been pre-cultured for 72 hr in DMEM containing 10% FBS, $^{13}C_3$-labeled downstream metabolites of glycolysis (GAP, dihydroxyacetone phosphate [DHAP], 2,3-bisphosphoglyceric acid [2,3BPG], 3-phosphoglyceric acid [3PG], 2-phosphoglyceric acid [2PG], and phosphoenolpyruvate [PEP]) were detected (Figure 1G). Thymidine-derived metabolites ($^{13}C_5$-DR5P and $^{13}C_3$-lactate) also accumulated in endogenous TP-expressing pancreatic cancer Panc1 and Yumoto cells (Figure S2D); the accumulation was suppressed upon *TP* small interfering RNA (siRNA) knockdown (Figure S2D). Although the pattern of ^{13}C-labeled metabolites varies depending on $^{13}C_5$-thymidine tracing times, cell culture conditions, or cell types, these results demonstrated that thymidine catabolism can act as a carbon source for glycolytic intermediates. Notably, $^{13}C_2$-*N*-acetylaspartic acid and $^{13}C_2$-*N*-acetylglutamic acid were observed in $^{13}C_5$-thymidine-treated KB/TP cells (Figure S2E), and DR5P-derived acetaldehyde is expected to react with amino acids to generate *N*-acetylamino acids. In $^{13}C_2$-acetaldehyde-treated KB/TP cells, the $^{13}C_2$-labeled *N*-acetylamino acid was detected (Figure S2F). These results strongly suggest that $^{13}C_5$-DR5P is converted to $^{13}C_3$-GAP and $^{13}C_2$-acetaldehyde by DERA.

DERA is a key enzyme in the pathway by which thymidine-derived DR5P enters the glycolytic pathway (Figure 1E). We examined the effect of DERA downregulation (Figure S2G) on ^{13}C-labeled DR5P in $^{13}C_5$-thymidine-treated KB/TP cells and the growth of KB/CV and KB/TP cells under serum-free conditions. siRNA-mediated *DERA* knockdown increased $^{13}C_5$-DR5P accumulation (Figure 1H) and significantly reduced viable in KB/TP cells cultured for 4 days under serum-free conditions (Figure 1I).

Utilization of Thymidine in KB Cells in Different Nutritional States

As shown in Figure 1A, the growth rates of KB cells cultured for 4–6 days in serum-free medium declined. The glucose and glutamine levels in the KB cell culture medium at 4 and 6 days were conspicuously lower than those in fresh medium (Figure S1D).

Figure 1. Growth Advantage by TP under Low-Nutrient Conditions

(A) Growth curves for KB/CV, KB/TP, and KB/TPmut cells in serum-free medium with or without 300 μM TPI.

(B) Colony-forming abilities of KB/CV and KB/TP cells. Shown are representative culture plates (left) and average colony counts calculated from three independent experiments (right).

(C) Effect of TPI on KB/CV and KB/TP colony formation in the absence or presence of 1.5 mM 2-DG.

(D) Cytotoxic effect of 2-DG with or without TPI on Yumoto cells incubated in serum-free medium in the absence or presence of TPI and/or 2-DG for 6 days.

(E) Catabolic pathway of $^{13}C_5$-thymidine.

(F) KB/CV and KB/TP cells were incubated in serum-free medium with 500 μM $^{13}C_5$-thymidine for the indicated times; ^{13}C-labeled metabolite levels were determined using CE-MS.

(G) KB/TP cells were treated with 500 μM $^{13}C_5$-thymidine for 1 hr after the cells were pre-cultured in DMEM containing 10% FBS for 72 hr.

(H) KB/TP cells transfected with *DERA* siRNA were treated with 500 μM $^{13}C_5$-thymidine for 1 hr; intracellular ^{13}C-labeled DR5P was determined.

(I) Effect of *DERA* knockdown on the survival of KB cells incubated for 4 days under serum-free conditions.

Data are represented as the means ± SD. *$p < 0.01$, **$p < 0.05$.

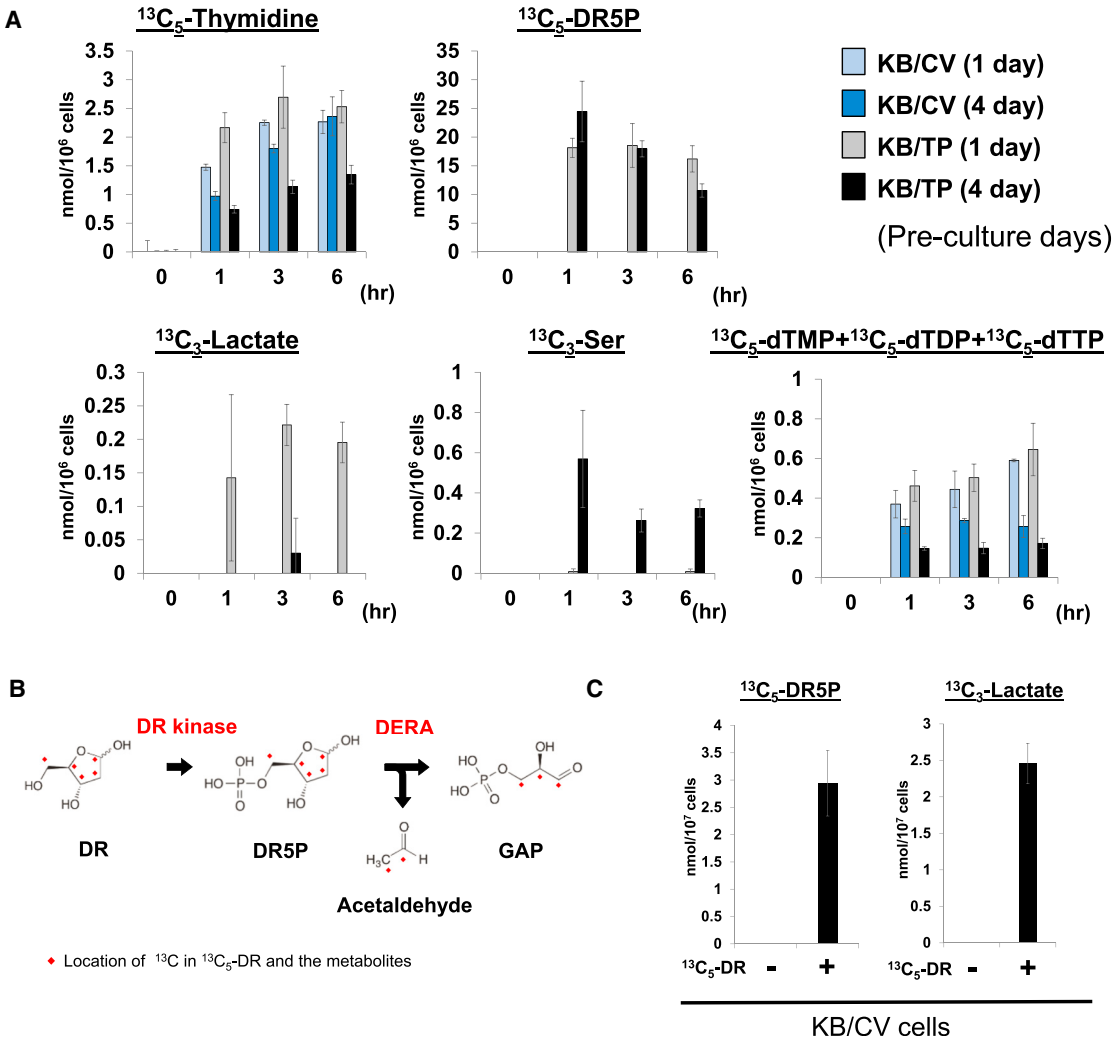

Figure 2. Metabolic Analysis of ^{13}C-Metabolites after Addition of $^{13}C_5$-Thymidine under Low-Nutrition Conditions

(A) KB/CV and KB/TP cells were treated with 500 μM $^{13}C_5$-thymidine for the indicated times after the cells were pre-cultured in serum-free medium for 1 or 4 days. ^{13}C-metabolite levels were determined using CE-MS.

(B) Catabolic pathway for $^{13}C_5$-DR.

(C) KB/CV cells were incubated in serum-free medium with 1 mM $^{13}C_5$-DR for 1 hr; ^{13}C-labeled metabolite levels were determined using CE-MS.

Data are represented as the means ± SD.

To examine thymidine catabolism in KB cells under low-nutrition conditions, we analyzed the $^{13}C_5$-thymidine-derived metabolites in KB cells pre-cultured with serum-free medium for 1 or 4 days. Figure 2A shows the time-dependent accumulation of $^{13}C_5$-thymidine and the thymidine-catabolized ^{13}C-metabolites (DR5P, lactate, and serine [Ser]) in KB cells treated with $^{13}C_5$-thymidine for the indicated times. Figure S3A indicates the enrichment of ^{13}C-metabolites in the same experiments. $^{13}C_5$-DR5P, $^{13}C_3$-lactate, and $^{13}C_3$-Ser were detected in KB/TP but not KB/CV cells. In KB/TP cells pre-cultured with serum-free medium for 4 days, $^{13}C_5$-thymidine was mainly metabolized to $^{13}C_3$-Ser. The $^{13}C_3$-Ser levels were suppressed by *DERA* siRNA (Figure S3B). Ser is derived from the glycolytic intermediate 3-phosphoglyceric acid via a three-step reaction and contributes to the survival of cancer cells (Yang and Vousden, 2016). This result implies that the thymidine-derived Ser serves the survival of KB/TP cells under low-nutrition conditions. Furthermore, we examined the ^{13}C-labeled thymidine phosphates (thymidine monophosphate [dTMP], thymidine diphosphate [dTDP], and thymidine triphosphate [dTTP]) to assess the utilization of $^{13}C_5$-thymidine for DNA synthesis in KB cells. (Figures 2A and S3A). The total ^{13}C-metabolite levels in dTMP, dTDP, and dTTP in KB/CV and KB/TP on day 4 were lower than those on day 1. Furthermore, the ^{13}C-metabolite levels in KB/TP on day 4 were lower than those in KB/CV on day 4. These results suggest that thymidine catabolism is needed for the survival of cancer cells under low-nutrition conditions.

Incorporation of Non-phosphorylated DR in Non-TP-Expressing Cancer Cells

Non-phosphorylated DR is secreted by TP-expressing cells, promotes endothelial and cancer cell migration (Bijnsdorp et al., 2010; Hotchkiss et al., 2003; Nakajima et al., 2004), and can be converted to DR5P by DR kinase in *Salmonella typhimurium* (Hoffee, 1968). We examined whether ^{13}C-labeled DR ($^{13}C_5$-DR) was converted to DR5P and consequently entered glycolysis in TP-negative cell lines: KB/CV, human umbilical vein endothelial cells (HUVECs), and human fibroblast MRC5 cells. Figure 2B shows the expected $^{13}C_5$-DR catabolic pathway. $^{13}C_5$-DR5P and $^{13}C_3$-lactate were detected in KB/CV cells treated for 1 hr (Figure 2C) but not in HUVECs and MRC5 cells (data not shown). These results suggest that DR secreted from TP-expressing cells is incorporated into adjacent, non-TP-expressing cancer cells as a carbon source for glycolysis. We also considered that the uptake or metabolism of DR might vary by cell type.

Metabolic Alterations by TP under Physiological Conditions

We next examined whether TP-mediated thymidine catabolism affects glycolytic pathway intermediates under physiological conditions. Previously, we established TP and uridine phosphorylase (UP) double knockout (TP-UP DKO) mice (because murine UP also exhibits TP activity) to abolish TP enzymatic activity (Haraguchi et al., 2002). We performed a metabolome analysis of the livers, which exhibit high TP activity (Haraguchi et al., 2002), from wild-type (WT) and TP-UP DKO mice, identifying and quantifying 236 metabolites (Table S1). Principal-component analysis (PCA) demonstrated differing characteristic patterns of metabolites levels in TP-UP DKO versus WT mouse livers (Figure 3A), with 56 differing significantly (Figure S4A). Metacore software analysis identified 10 canonical pathways that differed significantly between groups (Figure 3B); in particular, glycolysis and its adjacent pathways, including PPP and the tricarboxylic acid (TCA) cycle, were affected by TP. Hierarchical clustering heatmap analysis of glycolysis intermediates also showed different clustering between WT and TP-UP DKO mice (Figure 3C) and indicated significant changes in the majority of the intermediates (Figure S4B). We also tested whether $^{13}C_5$-thymidine was converted to glycolytic pathway intermediates in xenografted TP-expressing Yumoto cells and in the spleen and liver of tumor-bearing mice because high TP activity was detected in the liver but not in the spleen (Haraguchi et al., 2002). Figure 3D shows the $^{13}C_5$-thymidine concentrations in whole blood harvested 0, 3, and 10 min following tail vein injection in the mice. We identified higher $^{13}C_5$-thymidine levels in the spleen than in the liver and tumor tissues (Figure 3E, left) and the converse effect for $^{13}C_3$-lactate (Figure 3E, right). We also performed $^{13}C_5$-thymidine trace experiments in TP-UP DKO and WT mouse livers. The livers were harvested 3 min after $^{13}C_5$-thymidine injection. The $^{13}C_5$-thymidine levels in TP-UP DKO mouse livers were higher than those in WT mouse livers, whereas $^{13}C_3$-lactate exhibited the opposite trend (Figure 3F). These results demonstrate that thymidine-derived metabolites enter the glycolytic pathway in a physiological context and that thymidine catabolism depends on TP activity.

Levels of Thymidine and Phosphorylated Deoxyribose in Human Gastric Cancer

We reanalyzed our previously reported gastric cancer tissue metabolome data (Hirayama et al., 2009) and compared thymidine and phosphorylated deoxyribose (DR1P plus DR5P [DRP]) levels in tumor versus adjacent non-neoplastic tissues. Thymidine levels were significantly lower in tumors than in adjacent tissues (Figure 4A, left) and were negatively correlated with DRP, which showed the opposite pattern (Figures 4A, right, and 4B). These results suggest that thymidine catabolism activity is higher in tumors than in the adjacent non-neoplastic tissues.

DISCUSSION

Several bacteria can use the 2-deoxy-D-ribosyl moiety of 2′-deoxyribonucleosides as their sole carbon and energy source. Genetic and biochemical studies using *S. typhimurium* have shown that three enzymes, TP, PPM, and DERA, are involved in the thymidine catabolic pathway (Hoffee, 1968); however, equivalent mammalian studies are limited. TP/PD-ECGF expression in cancer, PPM in mammalian tissues, leukemia, and red blood cells (Accorsi et al., 1989; Nishida and Miyamoto, 1982), and DERA in vertebrate liver and numerous cell lines (Sgarrella et al., 1997) have been observed, implying that thymidine catabolism might satisfy mammalian cell carbon and energy requirements as well. In this study, we demonstrated thymidine catabolism in mammalian cells and its functions in cancer cells. However, our investigation of the biological implications of thymidine catabolism in energy metabolism in cancer cells is not yet complete. The tracing experiment of $^{13}C_5$-thymidine (Figure 2A) suggests that thymidine catabolism contributes to Ser biosynthesis and, consequently, confers resistance to nutrient starvation. In the future, we will be focusing on the role of thymidine-derived Ser in cancer cells.

The TP gene (*TYMP*) is also known as the causative gene for mitochondrial neurogastrointestinal encephalopathy (MNGIE) which is a severe autosomal recessive disease with a particularly poor prognosis (Hirano et al., 2012; Nishino et al., 1999). Previous reports suggested that the TP deficiency in MNGIE increases intracellular thymidine levels and leads to deoxynucleoside triphosphate pool imbalances, which, in turn, cause mitochondrial DNA instability (Hirano et al., 2012). On the other hand, we showed that the deficiency in TP enzymatic activity in mice resulted in alterations in glycolytic intermediates in liver tissues. These findings might instead represent the key phenotype through which the abnormality in glycolysis contributes to the pathogenesis of MNGIE.

In this study, the observed tumor glucose concentrations were significantly lower than previously reported (Gatenby et al., 2007) or in adjacent non-neoplastic gastric tissues (Hirayama et al., 2009). Elevated thymidine concentrations within the tumor microenvironment can occur because of necrotic cell DNA hydrolysis (Brown et al., 2000), and TP is overexpressed proximal to necrotic tissue in human breast cancer MD231 xenograft tumors (Griffiths et al., 1997). However, because the gastric cancer tissues used in this study did not contain necrotic regions, their thymidine and glucose levels were decreased, whereas their DRP levels were elevated compared with normal tissues. These

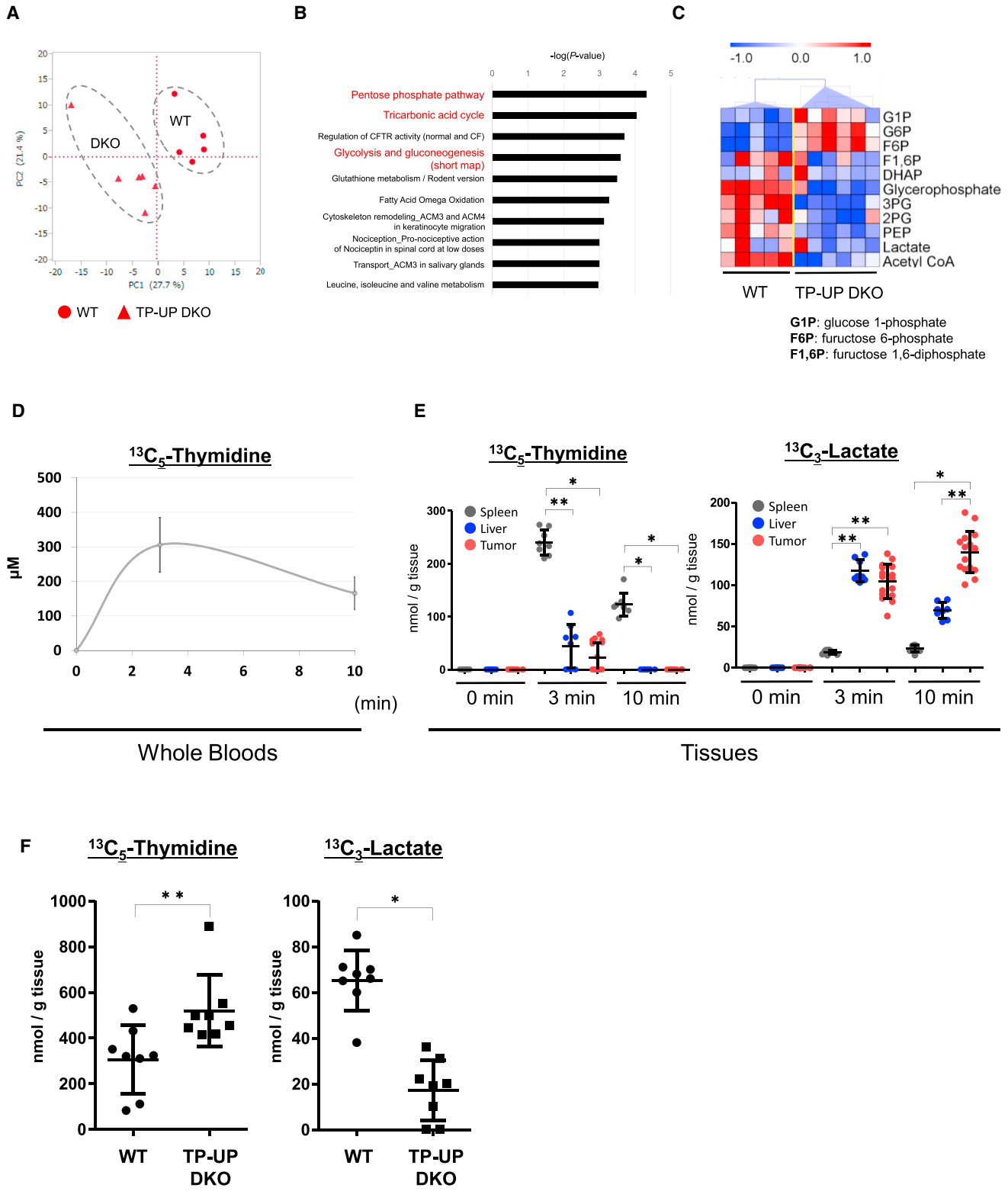

Figure 3. Thymidine Catabolism to Glycolysis in Physiological Contexts

(A) Score plots of PCA for metabolomics profiles of liver tissues in WT (n = 5) and TP-UP DKO mice (n = 6). Metabolite levels were detected with CE-MS.

(B) The first ten most altered liver tissue metabolic pathways in TP-UP DKO mice. Pathway significance was assessed using p values and FDRs (< 0.05).

(legend continued on next page)

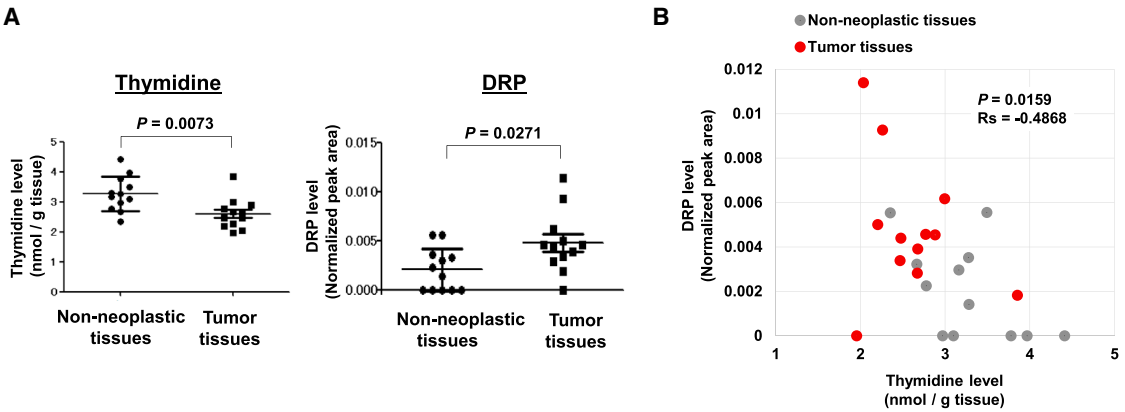

Figure 4. Thymidine and DRP Levels in Human Gastric Cancer

(A) Thymidine and DRP levels in human gastric cancer tissues and adjacent non-neoplastic tissues detected with CE-MS.

(B) Correlation between thymidine and DRP levels in the tissues.

Data are represented as the means ± SD.

results suggest that thymidine-derived DRP is consumed for glycolysis in tumors and that thymidine catabolism might be important for cancer cell survival in low-glucose microenvironments close to necrotic areas.

Inhibition of TP activity via agents such as TPI (Matsushita et al., 1999) and 6-(2-aminoethyl) amino-5-chlorouracil (Lu et al., 2009) or compounds that suppress thymidine-derived metabolite entry into the glycolytic pathway represents a potential novel anticancer strategy. Lu et al. (2009) reported that the combination of the vascular endothelial growth factor (VEGF) trap, a soluble VEGF decoy receptor, and a TP inhibitor exhibited additive antitumor activity that was significantly greater than VEGF inhibition alone. Recent studies also demonstrate the resistance to anti-angiogenic therapies caused by metabolic symbiosis (Allen et al., 2016; Jiménez-Valerio et al., 2016; Pisarsky et al., 2016), suggesting that TP might represent a suitable target to overcome such resistance.

A randomized phase 3 study of TAS102, a mixture of TPI and trifluorothymidine (TFT), an anticancer agent (Mayer et al., 2015), demonstrated improved overall survival and reduced the mortality of patients with metastatic colorectal cancer. Because TPI is thought to enhance TFT antitumor effects by inhibiting TP-dependent TFT degradation, consequently increasing its plasma levels, it might also abrogate the TP-mediated tumor growth advantage and angiogenic activity.

EXPERIMENTAL PROCEDURES

Chemicals and Cell Culture

$^{13}C_5$-thymidine and $^{13}C_5$-2-deoxy-D-ribose were obtained from Omicron Biochemicals. $^{13}C_2$-acetaldehyde was obtained from Cambridge Isotope Laboratory. 2-Deoxy-D-glucose was purchased from Sigma-Aldrich. Human epidermoid carcinoma KB, human bladder cancer EJ, human cervical carcinoma Yumoto, and human pancreatic cancer Panc1 cells were grown in DMEM (Nissui Seiyaku) containing 10% FBS, 2 mM glutamine, and 100 units/mL penicillin at 37°C in a 5% CO_2 humidified atmosphere.

Stable Transfection of TP/PD-ECGF cDNA

We previously established the following stable cell lines: KB/CV, KB/TP, KB/TPmut, EJ/CV, and EJ/TP (Nakajima et al., 2004; Tabata et al., 2012). The TP/PD-ECGF full-length cDNA plasmid, the TP/PD-ECGF mutant plasmid (L148R, Leu-148→Arg) (Miyadera et al., 1995), or the empty vector was transfected into KB or EJ cells by electroporation (Potter et al., 1984). After selection with geneticin, the expression of TP in each clone was determined by immunoblot analysis using an anti-TP monoclonal antibody as described previously (Takebayashi et al., 1996a).

Colony Formation Assay

Cells (2×10^2) were seeded in each well of a 6-well tissue culture plate and maintained in DMEM containing 10% FBS. The growth medium was changed every 3 days. After 7–14 days, the number of Giemsa-stained colonies was counted.

Relative colony counts were determined in three separate experiments with three wells each.

Cell Viability Assays

Equal numbers of cells (1×10^5) in 3 mL culture medium were inoculated in each well of a 6-well tissue culture plate. Cell viability was assayed by trypan blue exclusion using a Vi-Cell cell viability analyzer (Beckman Coulter).

Metabolite Quantification in Cells Using CE-MS

Intracellular metabolites were measured by capillary electrophoresis-time of flight-mass spectrometry (CE-TOFMS) (Agilent Technologies) as previously described (Uetaki et al., 2015). The data obtained were analyzed using MasterHands (Sugimoto et al., 2010). The metabolite identities were determined by matching their mass-to-charge ratio (*m/z*) values and migration times with those of their standard compounds.

(C) Heatmap showing the liver tissue glycolytic metabolite levels in WT (n = 5) and TP-UP DKO mice (n = 6). Metabolite levels in each sample were converted to a *Z* score. Red and blue indicate higher and lower levels, respectively, compared with the average (white).

(D) $^{13}C_5$-thymidine concentrations, measured with CE-MS, in whole-blood samples from tumor-bearing xenograft mice after $^{13}C_5$-thymidine injection (n = 7–8 for each point).

(E) $^{13}C_5$-thymidine and $^{13}C_3$-lactate levels in the spleen (n = 7–8), liver (n = 7–8), and tumor tissues (n = 14–16) from the xenograft mice.

(F) $^{13}C_5$-thymidine and $^{13}C_3$-lactate levels in the livers from WT (n = 8) and TP-UP DKO mice (n = 8).

Data are represented as the means ± SD. *$p < 0.01$, **$p < 0.05$.

Metabolome Analysis of the Livers from TP-UP DKO Mice

All animal experiments were approved by the Institutional Animal Care and Use Committee of Kagoshima University. The TP-UP DKO mouse strain was established previously (Haraguchi et al., 2002). Livers were collected from WT (n = 5) and TP-UP DKO female mice (8–10 weeks old) (n = 6) after blood removal. The excised tissues were immediately frozen in liquid nitrogen and stored at −80°C until use. The extraction and quantification of metabolites using capillary electrophoresis-mass spectrometry (CE-MS) were performed as described previously (Hirayama et al., 2009).

Analysis of Thymidine-Derived Metabolites in TP-UP DKO Mouse Livers

We utilized 8- to 10-week-old female mice in this study. Livers were extracted from WT (n = 8) and TP-UP DKO mice (n = 6) injected with $^{13}C_5$-thymidine (100 mg/kg intravenously [i.v.]). The livers were harvested 3 min after the $^{13}C_5$-thymidine injections. The excised livers were immediately frozen in liquid nitrogen and stored at −80°C until use. The extraction and quantification of metabolites using CE-MS were performed as described previously (Hirayama et al., 2009).

Xenograft Studies

Yumoto cells (1×10^6) were injected subcutaneously into both flanks of 6- to 8-week-old female athymic nude mice (CLEA Japan). After 4 weeks, whole blood, spleens, livers, and tumors were extracted from tumor-bearing mice injected with $^{13}C_5$-thymidine (100 mg/kg i.v.). The blood and tissues were harvested 0, 3, and 10 min after the $^{13}C_5$-thymidine injections. The excised tissues were immediately frozen in liquid nitrogen and stored at −80°C until use. The extraction and quantification of metabolites using CE-MS were performed as described previously (Hirayama et al., 2009).

Metabolite Quantification of Gastric Cancer Tissues Using CE-MS

We reanalyzed the levels of thymidine and DRP in gastric cancer tissues using our previously reported MS datasets (Hirayama et al., 2009). Samples were removed surgically at the National Cancer Center Hospital East; tumor and surrounding grossly normal-appearing tissues were collected after informed consent had been obtained from the patients according to the study protocol approved by the Institution Review Board of the National Cancer Center. The patient information and the tumor stages were described previously (Hirayama et al., 2009). The excised tissues were cut into <1-cm^3 pieces, immediately frozen in liquid nitrogen, and stored at −80°C until use. The extraction and quantification of metabolites using CE-MS were performed as described previously (Hirayama et al., 2009).

PCA and Heatmap Visualization

Principle-component analysis (PCA) and heatmap visualization were performed as described previously (Saito et al., 2013). PCA, which is a type of unsupervised statistical analysis used widely as a statistical tool in metabolomics studies, was applied prior to the detailed data analysis (Sugimoto et al., 2012). We also visualized the glycolytic metabolites levels as a heatmap representation and performed hierarchical clustering analysis using a Pearson correlation. JMP version 9.0.2 (SAS Institute) and Mev TM4 software (version 4.7.4., Dana-Farber Cancer Institute) were used for PCA and heatmap analysis, respectively.

Pathway Analysis

The significantly altered metabolites ($p < 0.05$ with a false discovery rate [FDR] of 0.05) were analyzed for pathway enrichment using MetaCore (Genego) (Schuierer et al., 2010; Trushina et al., 2013). The pathway maps in MetaCore are defined metabolic cascades that have been experimentally validated and are widely accepted. Metabolite identifiers (Kyoto Encyclopedia of Genes and Genomes [KEGG] ID and compound name) were used for each metabolite. The p value from the hypergenometric test, generated by MetaCore, represents the enrichment of a certain metabolite in a pathway. $p < 0.05$ is indicative of significant enrichment. The ratio of altered metabolites in the pathway to the total number of metabolites in a pathway was also calculated. An FDR of 0.05 was also applied for pathway enrichment.

Statistical Analysis

Data were analyzed using GraphPad Prism v5.0 software. In in vitro experiments, data for two groups and more than two groups were analyzed using Student's t test and one-way ANOVA, respectively. In mouse experiments and clinical studies, data for two groups and more than two groups were analyzed using Mann-Whitney *U* and Kruskal-Wallis tests, respectively. The correlation between thymidine and DRP levels in Figure 4B was analyzed using Spearman's correlation. The data are presented as the means ± SD, and differences were considered statistically significant at $p < 0.05$.

SUPPLEMENTAL INFORMATION

Supplemental Information includes Supplemental Experimental Procedures, four figures, and three tables and can be found with this article online at http://dx.doi.org/10.1016/j.celrep.2017.04.061.

AUTHOR CONTRIBUTIONS

Conceptualization, S.T., Y.N., T.S., T.F., and S.A.; Metabolic analysis, S.T., A.H., M.O., H.E., M.T., and T.S.; Bioinformatics, S.T., A.H., and M.O.; Mouse experiments, S.T., M.Y., R.I., M. Haraguchi, K.K.,Y.S., K.M., and T.F.; Molecular biology experiments, S.T., H.G., T.K., A.M., A.S., and M. Hanibuchi; Ideas and critical comments, S.T., S.S., M.T., T.F., and S.A.; Writing, S.T., T.S., T.F., and S.A.; Supervision, Y.N., S.S., M.T., T.S., T.F., and S.A.

ACKNOWLEDGMENTS

We thank K. Endo, A. Ueno, K. Umetsu, K. Igarashi, H. Mitsuo, and T. Oka for technical assistance. We thank Drs. K. Miyadera, A. Tomoda, A. Nagashima, T. Nishihara, and T. Ishikawa for helpful discussions and insights, and Dr. Michael M. Gottesman for critical reading of the manuscript. This study was supported by Japan Society for the Promotion of Science KAKENHI Grants (JP15K10338, JP26870456, JP16K07121, JP22501048, JP26870576, and JP16K21361), the Research Support Foundation of The University of Tokushima and TAIHO Pharmaceutical Co., Ltd., and research funds from the Yamagata Prefecture Government and Tsuruoka City.

Received: April 15, 2016
Revised: March 12, 2017
Accepted: April 20, 2017
Published: May 16, 2017

REFERENCES

Accorsi, A., Piatti, E., Piacentini, M.P., Gini, S., and Fazi, A. (1989). Isoenzymes of phosphoglucomutase from human red blood cells: isolation and kinetic properties. Prep. Biochem. *19*, 251–271.

Akiyama, S., Furukawa, T., Sumizawa, T., Takebayashi, Y., Nakajima, Y., Shimaoka, S., and Haraguchi, M. (2004). The role of thymidine phosphorylase, an angiogenic enzyme, in tumor progression. Cancer Sci. *95*, 851–857.

Allen, E., Miéville, P., Warren, C.M., Saghafinia, S., Li, L., Peng, M.W., and Hanahan, D. (2016). Metabolic Symbiosis Enables Adaptive Resistance to Anti-angiogenic Therapy that Is Dependent on mTOR Signaling. Cell Rep. *15*, 1144–1160.

Bijnsdorp, I.V., Azijli, K., Jansen, E.E., Wamelink, M.M., Jakobs, C., Struys, E.A., Fukushima, M., Kruyt, F.A., and Peters, G.J. (2010). Accumulation of thymidine-derived sugars in thymidine phosphorylase overexpressing cells. Biochem. Pharmacol. *80*, 786–792.

Brown, N.S., Jones, A., Fujiyama, C., Harris, A.L., and Bicknell, R. (2000). Thymidine phosphorylase induces carcinoma cell oxidative stress and promotes secretion of angiogenic factors. Cancer Res. *60*, 6298–6302.

Furukawa, T., Yoshimura, A., Sumizawa, T., Haraguchi, M., Akiyama, S., Fukui, K., Ishizawa, M., and Yamada, Y. (1992). Angiogenic factor. Nature *356*, 668.

Gatenby, R.A., Smallbone, K., Maini, P.K., Rose, F., Averill, J., Nagle, R.B., Worrall, L., and Gillies, R.J. (2007). Cellular adaptations to hypoxia and acidosis during somatic evolution of breast cancer. Br. J. Cancer *97*, 646–653.

Griffiths, L., Dachs, G.U., Bicknell, R., Harris, A.L., and Stratford, I.J. (1997). The influence of oxygen tension and pH on the expression of platelet-derived endothelial cell growth factor/thymidine phosphorylase in human breast tumor cells grown in vitro and in vivo. Cancer Res. *57*, 570–572.

Haraguchi, M., Miyadera, K., Uemura, K., Sumizawa, T., Furukawa, T., Yamada, K., Akiyama, S., and Yamada, Y. (1994). Angiogenic activity of enzymes. Nature *368*, 198.

Haraguchi, M., Tsujimoto, H., Fukushima, M., Higuchi, I., Kuribayashi, H., Utsumi, H., Nakayama, A., Hashizume, Y., Hirato, J., Yoshida, H., et al. (2002). Targeted deletion of both thymidine phosphorylase and uridine phosphorylase and consequent disorders in mice. Mol. Cell. Biol. *22*, 5212–5221.

Hirano, M., Garone, C., and Quinzii, C.M. (2012). CoQ(10) deficiencies and MNGIE: two treatable mitochondrial disorders. Biochim. Biophys. Acta *1820*, 625–631.

Hirayama, A., Kami, K., Sugimoto, M., Sugawara, M., Toki, N., Onozuka, H., Kinoshita, T., Saito, N., Ochiai, A., Tomita, M., et al. (2009). Quantitative metabolome profiling of colon and stomach cancer microenvironment by capillary electrophoresis time-of-flight mass spectrometry. Cancer Res. *69*, 4918–4925.

Hoffee, P.A. (1968). 2-deoxyribose gene-enzyme complex in Salmonella typhimurium. I. Isolation and enzymatic characterization of 2-deoxyribose-negative mutants. J. Bacteriol. *95*, 449–457.

Hotchkiss, K.A., Ashton, A.W., and Schwartz, E.L. (2003). Thymidine phosphorylase and 2-deoxyribose stimulate human endothelial cell migration by specific activation of the integrins alpha 5 beta 1 and alpha V beta 3. J. Biol. Chem. *278*, 19272–19279.

Jiménez-Valerio, G., Martínez-Lozano, M., Bassani, N., Vidal, A., Ochoa-de-Olza, M., Suárez, C., García-Del-Muro, X., Carles, J., Viñals, F., Graupera, M., et al. (2016). Resistance to Antiangiogenic Therapies by Metabolic Symbiosis in Renal Cell Carcinoma PDX Models and Patients. Cell Rep. *15*, 1134–1143.

Lu, H., Klein, R.S., and Schwartz, E.L. (2009). Antiangiogenic and antitumor activity of 6-(2-aminoethyl)amino-5-chlorouracil, a novel small-molecule inhibitor of thymidine phosphorylase, in combination with the vascular endothelial growth factor-trap. Clin. Cancer Res. *15*, 5136–5144.

Matsushita, S., Nitanda, T., Furukawa, T., Sumizawa, T., Tani, A., Nishimoto, K., Akiba, S., Miyadera, K., Fukushima, M., Yamada, Y., et al. (1999). The effect of a thymidine phosphorylase inhibitor on angiogenesis and apoptosis in tumors. Cancer Res. *59*, 1911–1916.

Mayer, R.J., Van Cutsem, E., Falcone, A., Yoshino, T., Garcia-Carbonero, R., Mizunuma, N., Yamazaki, K., Shimada, Y., Tabernero, J., Komatsu, Y., et al.; RECOURSE Study Group (2015). Randomized trial of TAS-102 for refractory metastatic colorectal cancer. N. Engl. J. Med. *372*, 1909–1919.

Miyadera, K., Sumizawa, T., Haraguchi, M., Yoshida, H., Konstanty, W., Yamada, Y., and Akiyama, S. (1995). Role of thymidine phosphorylase activity in the angiogenic effect of platelet derived endothelial cell growth factor/thymidine phosphorylase. Cancer Res. *55*, 1687–1690.

Nakajima, Y., Gotanda, T., Uchimiya, H., Furukawa, T., Haraguchi, M., Ikeda, R., Sumizawa, T., Yoshida, H., and Akiyama, S. (2004). Inhibition of metastasis of tumor cells overexpressing thymidine phosphorylase by 2-deoxy-L-ribose. Cancer Res. *64*, 1794–1801.

Nishida, Y., and Miyamoto, T. (1982). Properties and activities of phosphoribomutase in the human leukemic cells. Int. J. Biochem. *14*, 961–963.

Nishino, I., Spinazzola, A., and Hirano, M. (1999). Thymidine phosphorylase gene mutations in MNGIE, a human mitochondrial disorder. Science *283*, 689–692.

Pisarsky, L., Bill, R., Fagiani, E., Dimeloe, S., Goosen, R.W., Hagmann, J., Hess, C., and Christofori, G. (2016). Targeting Metabolic Symbiosis to Overcome Resistance to Anti-angiogenic Therapy. Cell Rep. *15*, 1161–1174.

Potter, H., Weir, L., and Leder, P. (1984). Enhancer-dependent expression of human kappa immunoglobulin genes introduced into mouse pre-B lymphocytes by electroporation. Proc. Natl. Acad. Sci. USA *81*, 7161–7165.

Saito, T., Sugimoto, M., Igarashi, K., Saito, K., Shao, L., Katsumi, T., Tomita, K., Sato, C., Okumoto, K., Nishise, Y., et al. (2013). Dynamics of serum metabolites in patients with chronic hepatitis C receiving pegylated interferon plus ribavirin: a metabolomics analysis. Metabolism *62*, 1577–1586.

Schuierer, S., Tranchevent, L.C., Dengler, U., and Moreau, Y. (2010). Large-scale benchmark of Endeavour using MetaCore maps. Bioinformatics *26*, 1922–1923.

Seeliger, H., Guba, M., Koehl, G.E., Doenecke, A., Steinbauer, M., Bruns, C.J., Wagner, C., Frank, E., Jauch, K.W., and Geissler, E.K. (2004). Blockage of 2-deoxy-D-ribose-induced angiogenesis with rapamycin counteracts a thymidine phosphorylase-based escape mechanism available for colon cancer under 5-fluorouracil therapy. Clin. Cancer Res. *10*, 1843–1852.

Sgarrella, F., Poddie, F.P., Meloni, M.A., Sciola, L., Pippia, P., and Tozzi, M.G. (1997). Channelling of deoxyribose moiety of exogenous DNA into carbohydrate metabolism: role of deoxyriboaldolase. Comp. Biochem. Physiol. B Biochem. Mol. Biol. *117*, 253–257.

Shimaoka, S., Matsushita, S., Nitanda, T., Matsuda, A., Nioh, T., Suenaga, T., Nishimata, Y., Akiba, S., Akiyama, S., and Nishimata, H. (2000). The role of thymidine phosphorylase expression in the invasiveness of gastric carcinoma. Cancer *88*, 2220–2227.

Sugimoto, M., Wong, D.T., Hirayama, A., Soga, T., and Tomita, M. (2010). Capillary electrophoresis mass spectrometry-based saliva metabolomics identified oral, breast and pancreatic cancer-specific profiles. Metabolomics *6*, 78–95.

Sugimoto, M., Kawakami, M., Robert, M., Soga, T., and Tomita, M. (2012). Bioinformatics Tools for Mass Spectroscopy-Based Metabolomic Data Processing and Analysis. Curr. Bioinform. *7*, 96–108.

Tabata, S., Ikeda, R., Yamamoto, M., Furukawa, T., Kuramoto, T., Takeda, Y., Yamada, K., Haraguchi, M., Nishioka, Y., Sone, S., and Akiyama, S. (2012). Thymidine phosphorylase enhances reactive oxygen species generation and interleukin-8 expression in human cancer cells. Oncol. Rep. *28*, 895–902.

Takebayashi, Y., Miyadera, K., Akiyama, S., Hokita, S., Yamada, K., Akiba, S., Yamada, Y., Sumizawa, T., and Aikou, T. (1996a). Expression of thymidine phosphorylase in human gastric carcinoma. Jpn. J. Cancer Res. *87*, 288–295.

Takebayashi, Y., Yamada, K., Miyadera, K., Sumizawa, T., Furukawa, T., Kinoshita, F., Aoki, D., Okumura, H., Yamada, Y., Akiyama, S., et al. (1996b). The activity and expression of thymidine phosphorylase in human solid tumours. Eur. J. Cancer *32a*, 1227–1232.

Trushina, E., Dutta, T., Persson, X.M., Mielke, M.M., and Petersen, R.C. (2013). Identification of altered metabolic pathways in plasma and CSF in mild cognitive impairment and Alzheimer's disease using metabolomics. PLoS ONE *8*, e63644.

Uetaki, M., Tabata, S., Nakasuka, F., Soga, T., and Tomita, M. (2015). Metabolomic alterations in human cancer cells by vitamin C-induced oxidative stress. Sci. Rep. *5*, 13896.

Yang, M., and Vousden, K.H. (2016). Serine and one-carbon metabolism in cancer. Nat. Rev. Cancer *16*, 650–662.